

Encapsulated Alkaline-Earth Metallocenes. 2.¹ Triisopropylcyclopentadienyl Systems, [(C₃H₇)₃C₅H₂]₂Ae(THF)_n (Ae = Ca, Sr, Ba; n = 0-2), and the Crystal Structure of [(C₃H₇)₃C₅H₂]₂Ba(THF)₂

David J. Burkey, R. Allen Williams, and Timothy P. Hanusa*

Department of Chemistry, Vanderbilt University, Nashville, Tennessee 37235

Received September 22, 1992

Reaction of 2 equiv of KCp³ⁱ (Cp³ⁱ = 1,2,4-(C₃H₇)₃C₅H₂) with AeI₂ (Ae = Ca, Sr, Ba) in Et₂O, THF, or THF/toluene produces the metallocenes (Cp³ⁱ)₂Ae(THF)_n (n = 0-2) in high yields. Both the monosolvated and base-free (Cp³ⁱ)₂Ca(THF)_n species are isolated as oily materials that partially solidify on long standing, whereas the mono- and disolvated strontium and barium complexes are solids. The base-free strontocene is an oil, and the corresponding barocene is initially isolated as a wax that solidifies on standing for several weeks. These unusual physical properties are apparently related to the inability of certain metal/ligand combinations to pack efficiently in ionic lattices. All the metallocenes sublime or distill at or below 140 °C at 10⁻⁶ Torr. Crystals of (Cp³ⁱ)₂Ba(THF)₂ grown from THF/hexane are monoclinic, space group C2/c, with a = 13.95(1) Å, b = 14.577(8) Å, c = 18.661(9) Å, β = 104.28(4)°, and D_c = 1.200 g cm⁻³ for Z = 4. Least-squares refinement based on 1669 observed reflections led to a final R value of 0.068. The complex possesses a bent metallocene geometry and contains a crystallographically imposed 2-fold rotation axis passing through the barium. The average Ba-C and Ba-O(THF) distances are 3.03(2) and 2.77(1) Å, respectively, and the ring centroid-Ca-ring centroid angle is 132°. The *i*-Pr groups on the side of the metallocene away from the THF have rotated and lie nearly in line with the Cp rings. This allows the Cp³ⁱ rings to bend back to accommodate the THF ligands without undue steric crowding.

Introduction

The use of highly substituted cyclopentadienyl rings, such as tetraisopropylcyclopentadiene, will generate "encapsulated" metallocenes of the calcium subgroup metals Ca, Sr, and Ba.¹ These complexes display several physical properties that are strikingly different from metallocenes containing less bulky substituents. Among them are increased volatility and air stability and a greatly reduced tendency to form adducts with Lewis bases. These differences are most likely related to the ability of the isopropyl groups of the rings to interlock, forming "cages" around the metal centers.

To gain greater insight into the effect the number and shape of the ring substituents have on the encapsulation phenomenon, we have investigated the properties of metallocenes derived from the 1,2,4-triisopropylcyclopentadienyl anion. These were selected to determine whether there is a "threshold" of steric bulk that produces encapsulation or whether it is meaningful to speak of "degrees" of encapsulation. Such information is of considerable importance in the design of new ligands that would make the metallocenes more attractive as sources of the alkaline-earth ions in gas-phase or solution reactions.²⁻⁴

Experimental Section

General Considerations. All manipulations were performed with the rigid exclusion of air and moisture. Unless otherwise

(1) Part 1: Williams, R. A.; Tesh, K. F.; Hanusa, T. P. *J. Am. Chem. Soc.* 1991, 113, 4843-4851.

(2) Benac, M. J.; Cowley, A. H.; Jones, R. A.; Tasch, A. F., Jr. *Chem. Mater.* 1989, 1, 289-290.

(3) Hubert-Pfalzgraf, L. G. *Nouv. J. Chem.* 1987, 11, 663-675.

(4) Bradley, D. C. *Chem. Rev.* 1989, 89, 1317-1322.

noted, chemicals were handled with high-vacuum, Schlenk, or drybox techniques. Proton NMR spectra were obtained at 300 MHz with a Bruker NR-300 spectrometer and were referenced to the residual proton resonances of C₆D₆ (δ 7.15); carbon (¹³C) NMR spectra were recorded at 50.3 MHz on a Bruker NR-200 spectrometer and were referenced to the residual ¹³C resonances of C₆D₆ (δ 128.0); the latter are collected in Table I. Infrared data were obtained on a Perkin-Elmer 1430 spectrometer either as KBr pellets prepared as previously described¹ or as neat samples between sealed KBr plates. Elemental analyses were performed by Oneida Research Services, Whitesboro, NY. Consistent C/H analyses were difficult to obtain for several complexes; carbon content was low by as much as 6% in one case. No regular pattern could be found in the deviations (both solvated and unsolvated molecules were affected), and analyses for metals displayed far less deviation (max discrepancy of 0.84%). The difficulty in obtaining accurate C/H analyses seems endemic to several types of alkaline-earth compounds.⁵⁻⁸

Materials. Anhydrous calcium iodide, strontium iodide, and barium iodide (95%) were commercial samples (Strem Chemicals or Cerac) heated under vacuum to remove residual amounts of free iodine. KCp³ⁱ (Cp³ⁱ = 1,2,4-(C₃H₇)₃C₅H₂) was prepared as previously described.¹ Anhydrous diethyl ether was purchased from Aldrich and used as received. Other solvents for reactions were dried and degassed using standard methods.⁹ C₆D₆ was vacuum distilled from Na/K (22/78) alloy.

Synthesis of (Cp³ⁱ)₂Ca(THF). Into a 125-mL Erlenmeyer flask equipped with a magnetic stirring bar were added KCp³ⁱ

(5) McCormick, M. J.; Sockwell, S. C.; Davies, C. E. H.; Hanusa, T. P.; Huffman, J. C. *Organometallics* 1989, 8, 2044-2049.

(6) Sockwell, S. C.; Hanusa, T. P.; Huffman, J. C. *J. Am. Chem. Soc.* 1992, 114, 3393-3399.

(7) Vaartstra, B. A.; Huffman, J. C.; Streib, W. E.; Caulton, K. G. *Inorg. Chem.* 1991, 30, 121-125.

(8) Gardiner, M. G.; Hanson, G. R.; Junk, P. C.; Raston, C. L.; Skelton, B. W.; White, A. H. *J. Chem. Soc., Chem. Commun.* 1992, 1154-1156.

(9) Perrin, D. D.; Armarego, W. L. F. *Purification of Laboratory Chemicals*, 3rd ed.; Pergamon: Oxford, U.K., 1988.

Table I. ^{13}C NMR Data For $(\text{Cp}^{3i})_2\text{Ae}(\text{THF})_n$ Metallocenes

compd	ring C's	$\alpha\text{-C}_4\text{H}_8\text{O}$	$-\text{CHMe}_2$	$-\text{CH}_3$	$\beta\text{-C}_4\text{H}_8\text{O}$
$(\text{Cp}^{3i})_2\text{Ca}$	133.3		29.1	26.4	
	129.2		26.0	25.4	
	102.2				
$(\text{Cp}^{3i})_2\text{Ca}(\text{THF})$	130.1	69.1	29.0	26.9	26.3
	102.1		25.2	25.2	
$(\text{Cp}^{3i})_2\text{Sr}$	132.6		29.2	26.5	
	ca. 128 ^a		25.8	25.5	
	102.0				
$(\text{Cp}^{3i})_2\text{Sr}(\text{THF})$	101.7	69.4	29.2	26.8	26.3
			25.3	25.3	
$(\text{Cp}^{3i})_2\text{Sr}(\text{THF})_2$	101.7	68.8	29.2	26.9	26.4
			25.4	25.3	
$(\text{Cp}^{3i})_2\text{Ba}$	130.8		29.1	26.9	
	104.2		25.1	25.7	
$(\text{Cp}^{3i})_2\text{Ba}(\text{THF})$	103.4	68.9	29.2	26.8	26.1
			25.2	25.3	
$(\text{Cp}^{3i})_2\text{Ba}(\text{THF})_2$	103.0	68.4	29.3	26.8	26.2
			25.2	25.5	

^a Obscured by C_6D_6 peak.

(0.723 g, 3.14 mmol) and CaI_2 (0.453 g, 1.54 mmol), followed by 50 mL of toluene and 10 mL of THF. After being stirred for 12 h, the tan reaction mixture was allowed to settle; the yellow supernatant solution was separated from the gray KI precipitate via pipet. Subsequent removal of toluene/THF gave 0.62 g (81% yield) of a viscous yellow oil. On standing for several hours, it solidified into an oily, semicrystalline mass. Spectroscopic analysis revealed that the compound was the monosolvated calcium metallocene, $(\text{Cp}^{3i})_2\text{Ca}(\text{THF})$. This compound also could be obtained by dissolving $(\text{Cp}^{3i})_2\text{Ca}$ (see below) in THF, followed by removal of the THF under vacuum, to produce a yellow oily solid in quantitative yield. Anal. Calcd for $\text{C}_{32}\text{H}_{54}\text{CaO}$: C, 77.67; H, 11.00; Ca, 8.10. Found: C, 77.88; H, 11.04; Ca, 8.01. ^1H NMR (C_6D_6): δ 5.78 (s, 4H, ring $-\text{CH}$), 3.52 (t, $J = 6.5$ Hz, 4H, $\alpha\text{-C}_4\text{H}_8\text{O}$), 2.98–2.89 (two overlapping septets, 6H, $-\text{CHMe}_2$), 1.35–1.30 (two overlapping doublets, 28H $-\text{CH}_3$ and $\beta\text{-C}_4\text{H}_8\text{O}$), 1.23 (d, $J = 6.7$ Hz, 12 H, $-\text{CH}_3$). Principal IR bands (neat, cm^{-1}): 3053 (w), 2959 (s, v br), 1462 (m), 1379 (m), 1360 (m), 1324 (w), 1276 (m), 1176 (m), 1104 (m), 1032 (m, br), 987 (w), 876 (w), 792 (m), 682 (w). Extraction of $(\text{Cp}^{3i})_2\text{Ca}(\text{THF})$ into toluene and subsequent removal of the toluene under vacuum partially desolvates the metallocene to give species of the composition $(\text{Cp}^{3i})_2\text{Ca}(\text{THF})_x$, where x ranges from 0.66 to 0.74 (^1H NMR). Repeated toluene extraction does not remove additional THF from the metal center.

Synthesis of $(\text{Cp}^{3i})_2\text{Ca}$. Into a 125-mL Erlenmeyer flask equipped with a magnetic stirring bar were added KCp^{3i} (1.51 g, 6.55 mmol) and CaI_2 (0.95 g, 3.2 mmol), followed by 50 mL of diethyl ether. After the resulting golden yellow suspension was allowed to stir for 20 h, the ether was removed under vacuum to leave a sticky yellow solid. The solid was then extracted with 60 mL of hexane. The yellow extract was allowed to stand, and the supernatant liquid was separated from the remaining gray solid via pipet. Removal of the hexane under vacuum gave 1.00 g (73% yield) of the unsolvated calcium metallocene $(\text{Cp}^{3i})_2\text{Ca}$ as a yellow viscous oil. Upon standing a few days, soft, cloudy crystalline material formed in the oil. Anal. Calcd for $\text{C}_{32}\text{H}_{54}\text{Ca}$: C, 79.55; H, 10.97. Found: C, 78.23; H, 10.97. ^1H NMR (C_6D_6): δ 5.68 (s, 4H, ring $-\text{CH}$), 2.90–2.80 (m, 6H, $-\text{CHMe}_2$), 1.27 (d, $J = 7.1$ Hz, 24H, $-\text{CH}_3$), 1.15 (d, $J = 7.3$ Hz, 12H, CH_3). Principal IR bands (neat, cm^{-1}): 3059 (w), 2960 (vs), 2870 (s), 1462 (s), 1380 (m), 1360 (m), 1260 (m), 1176 (w), 1100 (m), 1032 (s, br), 794 (s), 682 (w). The compound is completely soluble in minimal amounts of ethereal and hydrocarbon solvents, including hexane. Spectroscopic analyses of both the initially formed oil and the partially crystallized material formed on standing were identical. The compound sublimes quantitatively at 140 °C and 10^{-6} Torr (sublimation begins at 100 °C and 10^{-6} Torr), giving a similar yellow, waxy material.

Synthesis of $(\text{Cp}^{3i})_2\text{Sr}(\text{THF})_n$. A 125-mL Erlenmeyer flask equipped with a magnetic stirring bar was charged with KCp^{3i}

(0.724 g, 3.14 mmol) and SrI_2 (0.522 g, 1.53 mmol). To this was added 40 mL of THF, and the resulting tan suspension was stirred for 24 h. The THF was then removed under vacuum, and the brown residue was extracted with 40 mL of toluene. The tan extract was allowed to stand, and the supernatant liquid was separated from the remaining gray solid via pipet. Removal of the toluene under vacuum left 0.67 g (81%) of solid off-white $(\text{Cp}^{3i})_2\text{Sr}(\text{THF})$. Anal. Calcd for $\text{C}_{32}\text{H}_{54}\text{SrO}$: C, 70.86; H, 10.03; Sr, 16.15. Found: C, 64.85; H, 9.16; Sr, 16.99. ^1H NMR (C_6D_6): δ 5.78 (s, 4H, ring $-\text{CH}$), 3.42 (t, $J = 6.5$ Hz, 4H, $\alpha\text{-C}_4\text{H}_8\text{O}$), 2.99 (septet, $J = 6.8$ Hz, 4H, $-\text{CHMe}_2$), 2.93 (septet, $J = 6.8$ Hz, 2H, $-\text{CHMe}_2$), 1.33–1.25 (several overlapping peaks, 40H, $-\text{CH}_3$ and $\beta\text{-C}_4\text{H}_8\text{O}$). Principal IR bands (KBr pellet, cm^{-1}): 3055 (w), 2962 (s), 2860 (s), 1458 (s), 1386 (m), 1369 (m), 1260 (w), 1178 (w), 1105 (m), 1036 (m), 889 (w), 800 (w), 793 (w), 675 (w), 596 (m), 580 (m). Addition of 10 mL of a 50/50 THF/hexane solution to the monosolvated strontium metallocene resulted in the immediate precipitation of a cream-colored solid. This solid was the disolvated metallocene, $(\text{Cp}^{3i})_2\text{Sr}(\text{THF})_2$. ^1H NMR (C_6D_6): δ 5.79 (s, 4H, ring $-\text{CH}$), 3.48 (t, $J = 6.5$ Hz, 8H, $\alpha\text{-C}_4\text{H}_8\text{O}$), 3.04–2.95 (two overlapping septets, 6H, $-\text{CHMe}_2$), 1.35–1.30 (several overlapping peaks, 44H, $-\text{CHCH}_3$ and $\beta\text{-C}_4\text{H}_8\text{O}$). Attempts at growing X-ray quality crystals of $(\text{Cp}^{3i})_2\text{Sr}(\text{THF})_2$ from 50/50 THF/hexane solutions were unsuccessful, perhaps owing to its low solubility. $(\text{Cp}^{3i})_2\text{Sr}(\text{THF})_2$ loses up to half a THF on standing over several days at room temperature.

Sublimation of $(\text{Cp}^{3i})_2\text{Sr}(\text{THF})$ in an attempt to obtain the unsolvated metallocene produces partially solvated species. Heating the compound under vacuum (10^{-6} Torr) to 120 °C causes the compound to melt; almost simultaneously, a yellow oil begins to supercool on a cold finger. This material solidifies somewhat overnight to a sticky yellow solid. An ^1H NMR spectrum of the yellow sublimate indicates its composition is approximately $(\text{Cp}^{3i})_2\text{Sr}(\text{THF})_{0.6}$.

Attempted Synthesis of $(\text{Cp}^{3i})_2\text{Sr}$ in Diethyl Ether. In a 125-mL Erlenmeyer flask equipped with a magnetic stirring bar, KCp^{3i} (0.80 g, 3.5 mmol) and SrI_2 (0.522 g, 1.53 mmol) were added, followed by 35 mL of diethyl ether. The resulting gray suspension was stirred for 24 h, and the ether was then removed under vacuum to yield a tan/gray solid. However, extraction of this solid with 60 mL of toluene yielded no metallocene product. Repeating the above procedure with larger amounts of diethyl ether gave the same result. The grayish-tan mixture remaining after the toluene extraction was determined to be unreacted KCp^{3i} and SrI_2 ; they could be used to form $(\text{Cp}^{3i})_2\text{Sr}(\text{THF})$ by the addition of THF as described above.

Preparation of $(\text{Cp}^{3i})_2\text{Sr}$. A 0.91-g sample of $(\text{Cp}^{3i})_2\text{Sr}(\text{THF})$ was desolvated by the toluene distillation method described previously.¹⁰ Evaporation of the remaining toluene by vacuum left 0.70 g (88%) of a yellow-brown viscous oil, which was identified spectroscopically as THF-free $(\text{Cp}^{3i})_2\text{Sr}$. The compound distills onto a cold finger at 120 °C and 10^{-6} Torr as a spectroscopically pure viscous yellow oil, which thickens, but does not solidify, on long standing (months). Anal. Calcd for $\text{C}_{28}\text{H}_{46}\text{Sr}$: C, 71.51; H, 9.86. Found: C, 70.97; H, 9.54. ^1H NMR (C_6D_6): δ 5.64 (s, 4H, ring $-\text{CH}$), 2.92–2.82 (m, 6H, $-\text{CHMe}_2$), 1.29 (d, $J = 6.8$ Hz, 12H, $-\text{CH}_3$), 1.21 (d, $J = 6.8$ Hz, 12H, $-\text{CH}_3$), 1.15 (d, $J = 6.9$ Hz, 12H, $-\text{CH}_3$). Principal IR bands (neat, cm^{-1}): 3059 (w), 2958 (s), 2866 (s), 1460 (s), 1389 (m), 1373 (m), 1264 (m), 1186 (w), 1110 (m), 1037 (m, br), 891 (w), 800 (s), 696 (w), 465 (m).

Synthesis of $(\text{Cp}^{3i})_2\text{Ba}(\text{THF})_n$. A 125-mL Erlenmeyer flask equipped with a magnetic stirring bar was charged with KCp^{3i} (0.493 g, 2.14 mmol) and BaI_2 (0.407 g, 1.04 mmol). To the flask was added 40 mL of THF, and the resulting gray suspension was stirred for 48 h. The THF was then removed under vacuum, and the gray residue was extracted with 60 mL of toluene. The yellow extract was allowed to stand, and the supernatant liquid was separated from the remaining gray solid via pipet. Removal of the toluene under vacuum left 0.43 g (70% yield) of a pale yellow

solid with a composition corresponding to $(\text{Cp}^{3i})_2\text{Ba}(\text{THF})$. Anal. Calcd for $\text{C}_{33}\text{H}_{54}\text{BaO}$: C, 64.19; H, 9.19; Ba, 23.19. Found: C, 59.84; H, 8.19; Ba, 22.88. $^1\text{H NMR}$ (C_6D_6): δ 5.68 (s, 4H, ring-CH), 3.43 (t, $J = 6.5$ Hz, 4H, $\alpha\text{-C}_4\text{H}_8\text{O}$), 2.98 (septet, $J = 6.8$ Hz, 4H, $-\text{CHMe}_2$), 2.91 (septet, $J = 6.8$ Hz, 2H, $-\text{CHMe}_2$), 1.35–1.23 (several overlapping peaks, 40H, $-\text{CH}_3$ and $\beta\text{-C}_4\text{H}_8\text{O}$). Principal IR bands (KBr pellet, cm^{-1}): 3057 (w), 2952 (vs, br), 2864 (s), 1458 (m), 1374 (m), 1357 (m), 1321 (w), 1277 (w), 1182 (m), 1102 (w), 1031 (m), 876 (w), 782 (s), 761 (w), 669 (m), 463 (m, br). Slow recrystallization of $(\text{Cp}^{3i})_2\text{Ba}(\text{THF})$ from a hot 50/50 THF/hexane mixture produces crystals of $(\text{Cp}^{3i})_2\text{Ba}(\text{THF})_2$ (mp 107–120 °C dec (with loss of solvent)), which were used for X-ray analysis. $^1\text{H NMR}$ of crystals (C_6D_6): δ 5.72 (s, 4H, ring-CH), 3.49 (t, $J = 6.5$ Hz, 8H, $\alpha\text{-C}_4\text{H}_8\text{O}$), 3.00 (septet, 4H, $-\text{CHMe}_2$), 2.94 (septet, 2H, $-\text{CHMe}_2$), 1.37–1.28 (several overlapping peaks, 44H, $-\text{CH}_3$ and $\beta\text{-C}_4\text{H}_8\text{O}$).

Repeated sublimation of $(\text{Cp}^{3i})_2\text{Ba}(\text{THF})$ produces partially solvated species. Heating the compound under vacuum (110 °C, 10^{-3} Torr) causes it to melt; the material starts to condense and supercool on a cold finger at this temperature but solidifies on standing overnight. $^1\text{H NMR}$ of the waxy white sublimate indicates its composition is approximately $(\text{Cp}^{3i})_2\text{Ba}(\text{THF})_{0.65}$. Resublimation of this material under the same conditions as above generates a new sublimate of composition $(\text{Cp}^{3i})_2\text{Ba}(\text{THF})_{0.54}$ ($^1\text{H NMR}$).

Preparation of $(\text{Cp}^{3i})_2\text{Ba}$. A mixture of 1.252 g of $(\text{Cp}^{3i})_2\text{Ba}(\text{THF})_2$ and 0.140 g of $(\text{Cp}^{3i})_2\text{Ba}(\text{THF})_{0.54}$ was desolvated by the toluene distillation method described previously.¹⁰ After evaporation of the remaining toluene under vacuum, an off-white waxy solid was left. As $^1\text{H NMR}$ indicated that a small amount of THF was retained, the material was sublimed onto a cold finger at 120 °C and 10^{-6} Torr, yielding 0.877 g (79% based on Ba) of a white waxy solid, identified as $(\text{Cp}^{3i})_2\text{Ba}$, mp 92–94 °C. Anal. Calcd for $\text{C}_{25}\text{H}_{46}\text{Ba}$: C, 64.67; H, 8.92; Ba, 26.41. Found: C, 64.60; H, 9.11; Ba, 26.68. $^1\text{H NMR}$ (C_6D_6): δ 5.59 (s, 4H, ring-CH), 2.94 (septet, 4H, $J = 6.9$ Hz, $-\text{CHMe}_2$), 2.83 (septet, 2H, $J = 6.8$ Hz, $-\text{CHMe}_2$), 1.29 (d, $J = 6.9$ Hz, 12H, $-\text{CH}_3$), 1.27 (d, $J = 6.9$ Hz, 12H, $-\text{CH}_3$), 1.24 (d, $J = 6.9$ Hz, 12H, $-\text{CH}_3$). Principal IR bands (KBr pellet, cm^{-1}): 2955 (vs, br), 2863 (vs), 1458 (m), 1376 (m), 1355 (m), 1178 (m), 1103 (m), 1027 (m), 805 (s), 798 (m), 792 (m), 785 (m), 774 (s), 670 (m).

X-ray Crystallography of $(\text{Cp}^{3i})_2\text{Ba}(\text{THF})_2$. Crystals of $(\text{Cp}^{3i})_2\text{Ba}(\text{THF})_2$ were grown from a 1/1 THF/hexane mixture. A suitable prism was located and sealed in a capillary tube. All measurements were performed at 20 ± 1 °C on a Rigaku AFC6S diffractometer with graphite-monochromated $\text{Mo K}\alpha$ radiation. Relevant crystal and data collection parameters for the present study are given in Table II.

Cell constants and an orientation matrix for data collection were obtained from a least-squares refinement using the setting angles of 25 carefully centered reflections; Delauney reduction indicated a C-centered monoclinic cell. Data collection was performed using a continuous ω -2 θ scan with stationary backgrounds. No decay was evident in the intensities of three representative reflections measured after every 150 reflections. Data were reduced to a unique set of intensities and associated s values in the usual manner. On the basis of systematic absences and a statistical analysis of intensity distribution, which supported an acentric space group, unsuccessful attempts were made to solve the structure in the space group Cc. However, the structure was readily solved and refined in the centric group C2/c (No. 15), which required the imposition of a 2-fold rotation axis on the molecule. The structure was solved by a combination of both Patterson and direct methods (MITHRIL and DIRDIF) and Fourier techniques. An empirical absorption correction using the program DIFABS was applied to the data. All non-hydrogen atoms were refined anisotropically.

As not all the hydrogen atoms were evident on a difference Fourier map, their positions were calculated using idealized geometries based on packing considerations and $d(\text{C-H}) = 0.95$ Å. The positions were fixed for the final cycles of refinement. The large thermal ellipsoids for the methyl groups on C(12)

Table II. Crystal Data and Summary of Data Collection for $(\text{Cp}^{3i})_2\text{Ba}(\text{THF})_2$

formula	$\text{C}_{36}\text{H}_{62}\text{BaO}_2$
fw	664.21
color of cryst	colorless
cryst dimens, mm	$0.90 \times 0.70 \times 0.60$
space group	C2/c
cell dimens (at 20 °C, 25 reflectns)	
a, Å	13.95(1)
b, Å	14.577(8)
c, Å	18.661(9)
β , deg	104.28(4)
V, Å ³	3677(7)
Z	4
D(calcd), g/cm ³	1.200
wavelength, Å	0.710 69
abs coeff, cm ⁻¹	11.04
type of scan	ω -2 θ
scan speed, deg/min (in ω)	4.0
scan width	$1.73 + 0.30 \tan \theta$
bkgd counting	stationary counts; peak/ bkgd counting time = 2/1
limits of data collectn, deg	$6 \leq 2\theta \leq 50$
total no. of reflectns collected	3545
no. of unique intensities	3394
no. with $F > 3.00\sigma(F)$	1669
R(F)	0.068
$R_w(F)$	0.076
goodness of fit	2.09
max Δ/σ in final cycle	0.02
max/min peak (final diff map), e/Å ³	0.96/−1.28

Table III. Fractional Coordinates and Isotropic Thermal Parameters (Å²) for the Non-Hydrogen Atoms in $(\text{Cp}^{3i})_2\text{Ba}(\text{THF})_2$

atom	x/a	y/b	z/c	B_{iso}^a
Ba(1)	0	0.06530(8)	$1/4$	3.45(5)
O(1)	−0.0911(8)	−0.0768(7)	0.1600(6)	6.9(5)
C(1)	0.152(1)	0.2015(9)	0.2330(9)	4.5(7)
C(2)	0.210(1)	0.123(1)	0.2454(9)	4.8(7)
C(3)	0.1792(9)	0.072(1)	0.1802(7)	4.3(6)
C(4)	0.103(1)	0.1210(8)	0.1304(8)	4.3(6)
C(5)	0.085(1)	0.2003(9)	0.1645(9)	4.6(7)
C(6)	0.290(1)	0.098(1)	0.313(1)	7(1)
C(7)	0.387(1)	0.139(1)	0.314(1)	11(1)
C(8)	0.264(2)	0.124(2)	0.382(1)	13(2)
C(9)	0.229(1)	−0.015(1)	0.162(1)	7(1)
C(10)	0.310(1)	0.005(1)	0.123(1)	10(1)
C(11)	0.152(2)	−0.079(1)	0.115(1)	10(1)
C(12)	0.015(1)	0.278(1)	0.130(1)	5.4(8)
C(13)	0.060(1)	0.364(1)	0.136(2)	23(2)
C(14)	−0.036(2)	0.256(2)	0.052(1)	19(2)
C(15)	−0.132(1)	−0.154(1)	0.187(1)	9(1)
C(16)	−0.159(1)	−0.218(1)	0.125(1)	9(1)
C(17)	−0.176(2)	−0.159(2)	0.057(1)	13(2)
C(18)	−0.118(2)	−0.082(1)	0.079(1)	11(1)

^a Isotropic values for those atoms refined anisotropically are calculated using the formula given by: Hamilton, W. C. *Acta Crystallogr.* **1959**, *12*, 609–610.

suggested that they might be disordered. A careful search of difference Fourier maps, however, did not reveal any peaks above 0.50 e/Å³ that could represent alternate locations for the atoms. The ellipsoids must either represent slight, unresolvable disorder or somewhat larger than normal thermal motion. A final difference map was featureless; the peak of greatest height was 1.20 Å from the barium. Positional parameters are provided in Table III; non-hydrogen bond distances and angles are summarized in Table IV.

Results and Discussion

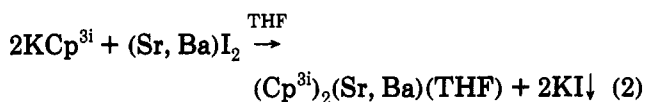
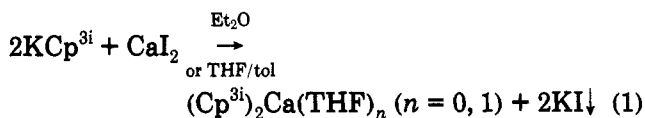
Synthesis of Triisopropylcyclopentadiene and KCp^{3i} . Although a variety of bulky cyclopentadienyl rings has been described in the literature, often the preparations

Table IV. Summary of Bond Distances (Å) and Angles (deg) in $(\text{Cp}^{3i})_2\text{Ba}(\text{THF})_2$

Ba-O(THF)	2.77(1)
O-Ba-O'	83.2(5)
Ba-C(ring) (av)	3.03(2)
Ba-ring centroid	2.79
ring centroid-Ba-ring centroid	131.7
planarity of Cp ring	within 0.02
C-C(Cp ring) (av)	1.39(4)
C(ring)-C(methine) (<i>i</i> -Pr group) (av)	1.52(3)
C(methyl)-C-C(methyl) (<i>i</i> -Pr group) (av)	110(3)

are tedious and the yields moderate to low.^{11,12} We recently reported that a method developed for the phase-transfer-catalyzed addition of *tert*-butyl groups to cyclopentadienyl rings¹³ could be modified to work with isopropyl groups as well.¹ The one-pot reaction of cyclopentadiene and 5 equiv of isopropyl bromide under basic conditions produces a mixture of products that is more than 70% triisopropylcyclopentadiene, the remainder being mainly the tetraisopropyl derivative. Crystals of potassium triisopropylcyclopentadienide (KCp^{3i}) are isolated on refluxing the hydrocarbon mixture with KH in THF. The NMR evidence for the isopropyl substitution pattern was not completely definitive, but the crystallographic characterization of $(\text{Cp}^{3i})_2\text{Ba}(\text{THF})_2$ (see below) established the 1,2,4-substitution pattern for the triisopropylcyclopentadienyl ion. This is the product that one would expect to dominate from steric considerations.

Metallocene Synthesis. The reaction of 2 equiv of KCp^{3i} with either calcium, strontium, or barium diiodides in Et_2O (Ca), THF (Sr, Ba), or THF/toluene (Ca) produces the metallocenes $(\text{Cp}^{3i})_2\text{Ae}(\text{THF})_n$ in >70% yield (eqs 1 and 2). The physical properties of the metallocenes vary

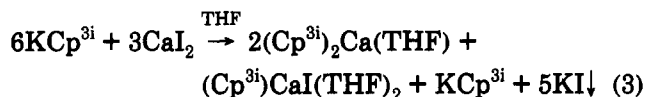


dramatically depending on the particular metal center and whether coordinated THF is present; they are therefore conveniently discussed separately for each metal.

Calcium Metallocenes. As initially isolated from THF/toluene solution, the calcium metallocene is coordinated to one THF molecule and is a yellow oily solid. No more than one THF is ever observed per metal center. Toluene extraction yields similar oily solids with THF content ranging from roughly two-thirds to three-fourths of a THF per metal center. Repeated extractions do not reduce the THF content further.

Attempts to prepare the metallocene in THF alone lead to mixtures with the monoring species $(\text{Cp}^{3i})\text{CaI}(\text{THF})_2$ (eq 3); the two are not easily separated, even by hexane extraction.

Analogous results are observed with the Cp^{4i} ($\text{Cp}^{4i} = 1,2,3,4\text{-}(\text{C}_3\text{H}_7)_4\text{C}_5\text{H}$) ion.¹⁴ These findings suggest that the



monoring species are kinetically stabilized intermediates in the formation of the metallocenes. Apparently, some loss of coordinated THF from the monoring species is required for metallocene formation to occur with these bulky Cp derivatives. This process is inhibited in THF to the point that metallocene formation is incomplete. When the concentration of THF is reduced, as in the THF/toluene mixtures, loss of THF from any monoring species that might be transiently formed is now favorable enough that it reacts with the remaining $\text{K}(\text{Cp}^{ni})$ to form the metallocene completely. On the basis of this analysis, the fact that no monoring species are observed if the reactions are performed in diethyl ether (see below) may be attributed to its lower basicity than THF, which would lead to a more facile loss of solvent from a diethyl ether-stabilized monoring intermediate.¹⁵

The base-free metallocene can be obtained by reaction of KCp^{3i} and CaI_2 in diethyl ether. No evidence is seen for a solvated metallocene, even when it is first isolated from the ether solution. Apparently, the lower basicity and/or larger size of ether, as compared to THF, precludes the formation of a $(\text{Cp}^{3i})_2\text{Ca}(\text{OEt}_2)$ species. Like the solvated metallocene, base-free $(\text{Cp}^{3i})_2\text{Ca}$ is an oily substance that partially solidifies on standing (2–10 days). If gently stirred with a spatula, however, the material breaks up and resumes its oily appearance. Attempted low-temperature crystallization does not yield a solid. Evidently, the formation of stable ionic lattices from the combination of Ca^{2+} and Cp^{3i-} ions (with or without THF) is difficult.

The unusual physical properties of the calcocenes distinguish them from the decamethylmetallocene Cp^*Ca on the one hand,^{10,16,17} and the encapsulated complex $(\text{Cp}^{4i})_2\text{Ca}$ on the other.¹ Unlike Cp^*Ca , which forms a disolvated complex with THF (albeit one in which one THF is easily removed), no more than one THF is ever observed with $(\text{Cp}^{3i})_2\text{Ca}(\text{THF})$. In contrast, it has proven impossible to form even a monosolvated $(\text{Cp}^{4i})_2\text{Ca}$ complex.¹ The degree of maximum THF solvation observed in these metallocenes $(\text{Cp}^*\text{Ca}(\text{THF})_2) > (\text{Cp}^{3i})_2\text{Ca}(\text{THF}) > (\text{Cp}^{4i})_2\text{Ca}(\text{THF})_0$ is clearly related to the order of the expected steric bulk of the rings ($\text{Cp}^* < \text{Cp}^{3i} < \text{Cp}^{4i}$), which suggests that such bulk directly limits access to the metal centers. The fact that only a monosolvated form of $(\text{Me}_4\text{EtC}_5)_2\text{Ca}(\text{THF})$ is observed in the solid state indicates that despite the differences in number and size of substituents, the effective bulk of the Me_4EtC_5 and (*i*-Pr)₃C₅H₂ rings is roughly similar.⁶

Strontium Metallocenes. The reaction of KCp^{3i} and SrI_2 in THF, followed by toluene extraction, yields the

(15) It is possible, though unlikely, that differences in the sizes of THF and Et_2O could play some role in these reactions. An initially formed $(\text{Cp}^{3i})\text{Ca}(\text{Et}_2\text{O})$ species would have to lose the Et_2O completely to form the metallocene, whereas the more sterically compact THF ligand could remain on the metal center. This suggests that metallocene formation would be favored in THF, contrary to what is observed. The effect of solubility differences between possible intermediates and products is more difficult to gauge, especially given the differing degrees of solvation possible. It should be noted, however, that the reactions are driven primarily by the precipitation of KI, which is virtually insoluble in either THF or Et_2O .

(16) Burns, C. J.; Andersen, R. A. *J. Organomet. Chem.* 1987, 325, 31–37.

(17) McCormick, M. J.; Williams, R. A.; Levine, L. J.; Hanusa, T. P. *Polyhedron* 1988, 7, 725–730.

(11) Okuda, J. *Top. Curr. Chem.* 1992, 160, 97–145.

(12) Janiak, C.; Schumann, H. *Adv. Organomet. Chem.* 1991, 33, 291–393.

(13) Venier, C. G.; Casserly, E. W. *J. Am. Chem. Soc.* 1990, 112, 2808–2809.

(14) Burkey, D. J.; Alexander, E. K.; Williams, R. A.; Hanusa, T. P. Manuscript in preparation.

monosolvated species $(\text{Cp}^{3i})_2\text{Sr}(\text{THF})$. Unlike the calcium metallocenes, a disolvated $(\text{Cp}^{3i})_2\text{Sr}(\text{THF})_2$ species can be generated from $(\text{Cp}^{3i})_2\text{Sr}(\text{THF})$ by recrystallization from a 50/50 THF/toluene mixture. Both the mono- and disolvated versions are off-white solids. Evidently, the larger size of strontium provides enough room in its coordination sphere to accept the additional THF molecule. The observation that the second THF is partially lost (ca. 0.5 THF) on standing for several days, however, suggests that the metal center in $(\text{Cp}^{3i})_2\text{Sr}(\text{THF})_2$ is nearly oversaturated and will release THF to relieve steric crowding.¹⁸

Curiously, KCp^{3i} and SrI_2 do not react in diethyl ether to form the metallocene. This is unusual, as KCp^* (or KCp^{4i}) and SrI_2 will react in Et_2O to produce the corresponding metallocene, and as noted above, KCp^{3i} and CaI_2 react to form $(\text{Cp}^{3i})_2\text{Ca}$ in ether. Evidently, the low solubility of the $\text{KCp}^{3i}/\text{SrI}_2$ combination inhibits metathesis.

Sublimation only partially desolvates $(\text{Cp}^{3i})_2\text{Sr}(\text{THF})$ to produce a mixture of the mono- and unsolvated metallocenes. The coordinated THF can be removed completely by the ambient pressure "toluene reflux method" to yield the base-free material.¹ Unlike the solvated metallocene, but like $(\text{Cp}^{3i})_2\text{Ca}$, $(\text{Cp}^{3i})_2\text{Sr}$ is isolated as a viscous yellow oil that distills at 120 °C and 10^{-6} Torr. It thickens on long standing (>1 months) but never appears to form crystalline material.

Barium Metallocenes. As with the strontium analogue, the reaction of KCp^{3i} and BaI_2 in THF, followed by toluene extraction, initially yields a monosolvated species $(\text{Cp}^{3i})_2\text{Ba}(\text{THF})$. An attempt to grow crystals of $(\text{Cp}^{3i})_2\text{Ba}(\text{THF})$ from hot hexane failed. Crystallization of the material from 50/50 THF/hexane, however, produces spectacularly large (up to 7 mm long) crystals of $(\text{Cp}^{3i})_2\text{Ba}(\text{THF})_2$, suitable for study by X-ray diffraction.

Sublimation of $(\text{Cp}^{3i})_2\text{Ba}(\text{THF})$ produces only partially desolvated species, as was observed for the strontium analogue. Repeating the sublimation still does not remove all the coordinated THF. This is uncharacteristic behavior for Sr and Ba metallocenes, as all previously reported compounds of this type $(\text{Cp}^*_2\text{Ba},^{10} (t\text{-BuCp})_2\text{Sr}, (t\text{-BuCp})_2\text{Ba},^{19} ((\text{Me}_3\text{Si})_2\text{Cp})_2\text{Sr}, ((\text{Me}_3\text{Si})_2\text{Cp})_2\text{Ba}^{20})$ completely desolvate on sublimation. Part of the difference may be that $(\text{Cp}^{3i})_2(\text{Sr},\text{Ba})(\text{THF})$ melt as they volatilize; thus they distill at low pressures as the solvated metallocenes. The difficulty in removing THF also may be related to problems in forming stable lattices with the Cp^{3i-} and $\text{Sr}^{2+}/\text{Ba}^{2+}$ combination (note the change from solids to oils or waxes on loss of THF). Crystallization to form base-free species does not provide a strong driving force for extrusion of THF.

The solvated metallocene can be desolvated by the previously described toluene reflux method¹⁰ to produce the waxy base-free metallocene. The compound solidifies on long standing (weeks) to give an off-white powder. Attempted recrystallization of the powder from hexane at -40 °C yields only the waxy material on warming to room temperature. Although the desolvated $(\text{Cp}^{3i})_2\text{Ba}$ has a lower melting point than $(\text{Cp}^{4i})_2\text{Ba}$, it is not as volatile, subliming at 120 °C at 10^{-6} Torr (cf. 90 °C and 10^{-2} Torr

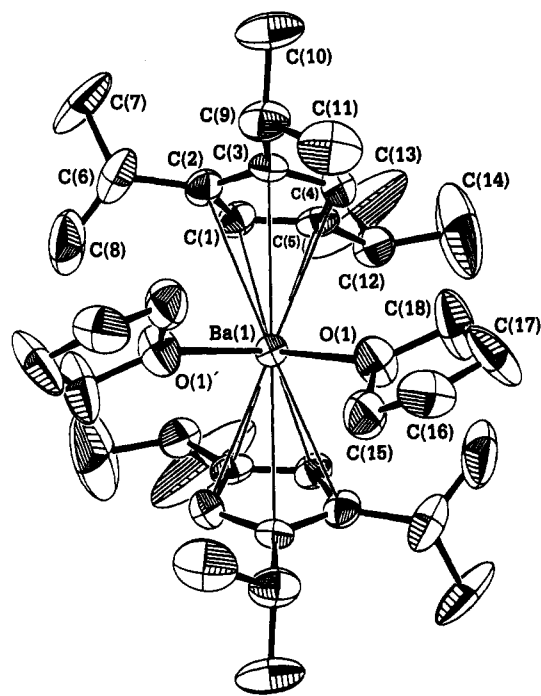


Figure 1. ORTEP view of $(\text{Cp}^{3i})_2\text{Ba}(\text{THF})_2$, giving the numbering scheme used in the tables. Thermal ellipsoids are shown at the 35% level, and the hydrogen atoms have been omitted for clarity.

for $(\text{Cp}^{4i})_2\text{Ba}$). Even so, $(\text{Cp}^{3i})_2\text{Ba}$ is somewhat more volatile than Cp^*_2Ba (135 °C, 10^{-4} Torr), despite the 16% increase in molecular weight.²¹

Unlike those of Cp^*_2Ba , solutions of $(\text{Cp}^{3i})_2\text{Ba}$ in aromatic solvents are colorless. This suggests the interaction with arenes that occurs with Cp^*_2Ba is blocked in the triisopropylcyclopentadienyl derivative.²²

X-ray Crystal Structure of $(\text{Cp}^{3i})_2\text{Ba}(\text{THF})_2$. $(\text{Cp}^{3i})_2\text{Ba}(\text{THF})_2$ crystallizes from a 50/50 THF/hexane mixture as large colorless slabs. It possesses a bent metallocene geometry, with two 1,2,4-triisopropylcyclopentadienyl rings bonding to the metal center and two THF ligands in a distorted tetrahedral geometry. The structure represents the first crystallographically characterized solvated barocene. Because of a crystallographically imposed C_2 axis through the barium atom, only half the molecule is unique. An ORTEP view of the complete molecule displaying the numbering scheme used in the tables is provided in Figure 1.

The average Ba-C distance of 3.03(1) Å is appreciably longer than that in $(\text{Cp}^{4i})_2\text{Ba}$ (2.94(1) Å)¹ but is in line with the 0.07-Å increase in radius expected on going from 6- to 8-coordinate Ba^{2+} .²³ As with $(\text{Cp}^{4i})_2\text{Ba}$, the individual molecules of $(\text{Cp}^{3i})_2\text{Ba}(\text{THF})_2$ are well separated in the solid state, with the shortest intermolecular contact at 3.70(4) Å (C(17)⋯C(17')). In contrast, intramolecular metal-ring contacts in Cp^*_2Ba that are only 0.28 Å longer than the longest intramolecular Ba-C distances (3.07 Å) generate one-dimensional coordination polymers in the lattice.¹⁰

The ring centroid-Ba-ring centroid angle of 131.7° in $(\text{Cp}^{3i})_2\text{Ba}(\text{THF})_2$ is only slightly larger than the analogous angle found in Cp^*_2Ba in the solid state (131.0°). Con-

(18) Evans, W. J. *Adv. Organomet. Chem.* 1985, 24, 131-177.

(19) Gardiner, M. G.; Raston, C. L.; Kennard, C. H. L. *Organometallics* 1991, 10, 3680-3686.

(20) Engelhardt, L. M.; Junk, P. C.; Raston, C. L.; White, A. H. *J. Chem. Soc., Chem. Commun.* 1988, 1500-1501.

(21) Hanusa, T. P. *Chem. Rev.*, in press.

(22) Williams, R. A.; Hanusa, T. P.; Huffman, J. C. *J. Organomet. Chem.* 1992, 429, 143-152.

(23) Shannon, R. D. *Acta Crystallogr.* 1976, A32, 751-767.

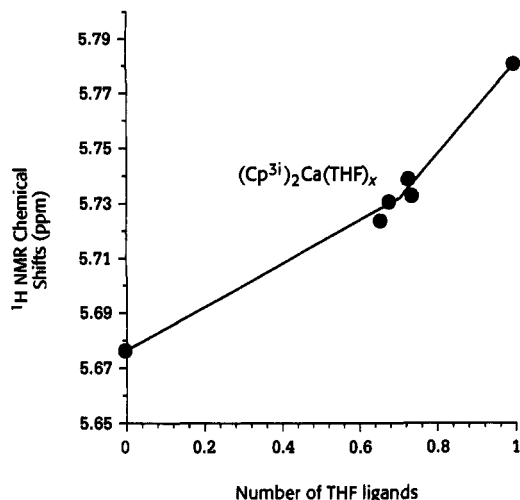


Figure 2. ^1H NMR chemical shifts (C_6D_6) of the ring protons of $(\text{Cp}^{3i})_2\text{Ca}(\text{THF})_x$, as x varies from 0 to 1.

sidering that Cp^*_2Ba lacks coligands to force a small angle, the similarity in the ring centroid–metal–ring centroid angles in these different barocenes is striking. Both angles are noticeably less than in the pyrazine-bridged complex $[\text{Cp}^*_2\text{Ba}]_2(\mu\text{-C}_4\text{H}_4\text{N}_2)$ (138°)²² or the $(\text{Cp}^{4i})_2\text{Ba}$ analogue (154.3°). More meaningful than a comparison of bending angles, however, is a ranking of the shortest intramolecular contacts in the molecules; on this basis, $(\text{Cp}^{3i})_2\text{Ba}(\text{THF})_2$ exhibits little evidence of crowding. The shortest separation in $(\text{Cp}^{3i})_2\text{Ba}(\text{THF})_2$ not involving THF is a ring–methine carbon contact at $4.02(2)$ Å ($\text{C}(1)\text{--}\text{C}(12')$), whereas the closest nonbonded intramolecular $\text{CH}_3\cdots\text{CH}_3'$ contacts in Cp^*_2Ba , $[\text{Cp}^*_2\text{Ba}]_2(\mu\text{-C}_4\text{H}_4\text{N}_2)$, and $(\text{Cp}^{4i})_2\text{Ba}$ occur at 3.49, 3.75, and 3.67 Å, respectively. The latter values are somewhat less than the sum of the appropriate van der Waals' radii (4.0 Å).²⁴

The freedom from congestion in $(\text{Cp}^{3i})_2\text{Ba}(\text{THF})_2$, especially as compared to $(\text{Cp}^{4i})_2\text{Ba}$, is a consequence of the removal of an isopropyl group from each cyclopentadienyl ring. The *i*-Pr groups on the side of the metallocene away from the THF are now free to rotate and thus lie nearly in line with the Cp rings (Figure 1). This is evident in a comparison of the planes formed by the two methyl carbons of the *i*-Pr groups and the adjacent ring carbons with the ring planes. In $(\text{Cp}^{4i})_2\text{Ba}$ these interplanar angles range from 48.3 to 90.0° , with an average of 77.0° .²⁵ In $(\text{Cp}^{3i})_2\text{Ba}(\text{THF})_2$, the isopropyl groups on the "front" and "side" of the complex ($\text{C}(10)\text{--}\text{C}(3)\text{--}\text{C}(11)$ and $\text{C}(7)\text{--}\text{C}(2)\text{--}\text{C}(8)$, respectively) are rotated by 67.4 and 67.7° about the ring plane, whereas that on the "back" ($\text{C}(13)\text{--}\text{C}(5)\text{--}\text{C}(14)$) makes an angle of only 29.9° to the plane. Rotation of the latter isopropyl groups allows the Cp^{3i} rings to bend back to accommodate the THF ligands without undue steric crowding.

NMR Chemical Shifts. It quickly became apparent during this study that the proton spectra of the metallocenes display significant differences in chemical shifts depending on the amount of THF present. This is particularly evident in the chemical shifts of the ring C–H protons (Figures 2 and 3). They exhibit a downfield shift of approximately 0.12 ppm as the THF content increases

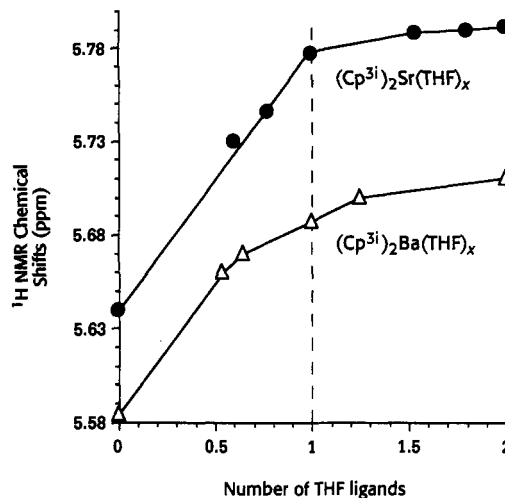


Figure 3. ^1H NMR chemical shifts (C_6D_6) of the ring protons of $(\text{Cp}^{3i})_2\text{Sr}(\text{THF})_x$ and $(\text{Cp}^{3i})_2\text{Ba}(\text{THF})_x$, as x varies from 0 to 2. The change in shift from 0 to 1 is substantially greater than that from 1 to 2.

from zero to one (for Ca, Sr, and Ba) and then a much smaller change (≤ 0.02 ppm) on changing from one to two (Sr and Ba). The minor effect of the second THF may reflect the fact that it is largely dissociated in solution, i.e., that THF exchange is occurring rapidly enough in C_6D_6 that on the average only slightly more than one THF is bound to the metal at any given time.

The shifts in the proton spectra of the metallocenes could stem from several causes.²⁶ It is likely that the addition of the coordinated THF will cause substantial changes in the solution structure of the metallocenes, such as an opening of the centroid–M–centroid angle or a rearrangement of the isopropyl groups on the ring. These structural changes might manifest themselves in the observed changes in the proton spectra. The increased electron density at the metal center upon THF complexation also could be responsible for the observed shifts.

It should be noted that a similar phenomenon has been observed in the chemical shifts of the barium amide $\{\text{Ba}[\text{N}(\text{SiMe}_3)_2]_2\}_n(\text{THF})_m$.⁷ The ^1H NMR trimethylsilyl resonance jumps from δ 0.19 to 0.26 ppm on going from the base-free ($n = 2$; $m = 0$) to the monosolvated species ($n = 2$; $m = 2$), though the solid-state structure of the compound does not undergo significant changes. It then moves only to δ 0.28 ppm in the disolvated amide ($n = 1$; $m = 2$), although the solid-state structure of the compound changes from a dimer to a monomer upon the addition of the second THF. This seems to indicate that it is the extra electron density at the metal center upon coordination of THF that is primarily responsible for the observed downfield shifts in the proton resonances in these compounds.

Unlike the proton spectra, the carbon (^{13}C) spectra of the metallocenes (Table I) do not show any definite trends based on the number of coordinated THF molecules at the metal center. The carbon spectra are further differentiated from the proton spectra in that only *two* resonances are seen for the methyl carbons of the Cp^{3i} ring, whereas *three* peaks are always seen for the corresponding methyl protons. Evidently, the solution behavior of the metallocenes is such that the methyl carbons at the 1 and

(24) Pauling, L. *The Nature of the Chemical Bond*, 3rd ed.; Cornell University Press: Ithaca, NY, 1960.

(25) This definition is slightly different from that given in ref 1. It should provide a more realistic estimate of the relative orientation of the *i*-Pr groups to the ring planes.

(26) We thank a reviewer for several of these suggestions.

2 positions of the cyclopentadienyl ring are equivalent on the NMR time scale, while the associated hydrogens are not.

It should be noted that this behavior is distinctly different from that observed with the Cp⁴ⁱ-based metallocenes: both ¹H and ¹³C NMR spectra show four separate resonances corresponding to the methyl protons and carbons of the isopropyl groups on the ring. This is possibly a result of the greater steric restrictions on isopropyl group rotation in the Cp⁴ⁱ ring in solution.

Implications for Encapsulation. The results presented here suggest that it is reasonable to consider the encapsulation of a metal center in an alkaline-earth metallocene as a variable phenomenon, with different features of encapsulation becoming evident at different levels of cyclopentadienyl steric bulk. This is most obvious in the discrimination displayed between the number and kind of coordinated bases that can be accepted on the metal centers. With increasing steric bulk of the ligands the number of THF ligands that can be coordinated to the metallocenes decreases, falling to zero in fully encapsulated species. Furthermore, the fact that two THF ligands can bind to (Cp³ⁱ)₂Ba (like Cp*₂Ba) whereas (Cp³ⁱ)₂Ba displays no interaction toward aromatic solvents (unlike Cp*₂Ba, but like (Cp⁴ⁱ)₂Ba) suggests that the *geometry* of the cyclopentadienyl rings plays a critical role in determining which bases will be allowed access to the metal center.

That a high degree of encapsulation is required to exclude small bases from the metal coordination sphere is evident from the air sensitivity of the (Cp³ⁱ)₂Ae complexes. Although (Cp⁴ⁱ)₂Ca can tolerate several minutes' exposure to air before noticeably decomposing,¹ the triisopropyl analogue decomposes within seconds on exposure to air. Since THF will bind to (Cp³ⁱ)₂Ca, it is reasonable to expect that facile attack by the much smaller base O₂ also should occur. The metal center in (Cp⁴ⁱ)₂Ca, which does not bind ethers, is evidently shielded enough from oxygen to inhibit (although not completely prevent) attack by O₂ and subsequent decomposition.

That the physical properties of the metallocenes and their relative sensitivity to bases and oxygen should be so

dependent on the presence or absence of a single isopropyl group on the Cp ring indicates that the difference between the Cp³ⁱ and Cp⁴ⁱ ligands is not a trivial one. Large variations in encapsulation effects can evidently arise from comparatively subtle changes in ligand design.

Conclusions

The phenomenon of metallocene "encapsulation", originally identified with calcium and barium derivatives of tetraisopropylcyclopentadiene, has been extended to triisopropylcyclopentadienyl analogues of the heavy alkaline-earth metals. Although these do not display the high levels of air stability and volatility found with the tetrasubstituted derivatives, they demonstrate that encapsulation can be accomplished by stages. With progressive increases in encapsulation, molecules become more volatile, less likely to form adducts with Lewis bases, and less air- and moisture-sensitive. Furthermore, the dramatically different physical characteristics seen for these metallocenes, especially when compared to other known compounds of this type, point out that the properties of organo-alkaline-earth compounds are much more susceptible to subtle changes in ligands than previously believed. This variability suggests that metallocenes and perhaps other classes of organoalkaline-earth molecules can be deliberately tuned by appropriate ligand choice to provide different levels of encapsulation and therefore greater control over their subsequent reactivity.

Acknowledgment is made to the U.S. Army Research Office for generous support of this work. A reviewer is acknowledged for helpful comments. D.J.B. is the grateful recipient of an NSF Predoctoral Fellowship. We thank Erik K. Alexander for experimental assistance.

Supplementary Material Available: Tables of hydrogen atom fractional coordinates, bond distances and angles involving hydrogen atoms, and anisotropic thermal parameters (3 pages). Ordering information is given on any current masthead page.

OM920582W